Communication

A Mixed-Valence Superstructure Assembled from A Mixed-Valence Host-Guest Complex

Zhichang Liu, Marco Frasconi, Wei-Guang Liu, Yu Zhang, Scott M. Dyar, Dengke Shen, Amy A. Sarjeant, William A. Goddard, Michael R. Wasielewski, and J. Fraser Stoddart

J. Am. Chem. Soc., **Just Accepted Manuscript** • DOI: 10.1021/jacs.8b05322 • Publication Date (Web): 27 Jun 2018

A Mixed-Valence Superstructure Assembled from A Mixed-Valence Host-Guest Complex

Zhichang Liu,[1,3,*] Marco Frasconi,[2] Wei-Guang Liu,[4] Yu Zhang,[1] Scott M. Dyar,[1] Dengke Shen,[1] Amy A. Sarjeant,[1] William A. Goddard III,[4] Michael R. Wasielewski,[1,5] and J. Fraser Stoddart[1,*]

[1]Department of Chemistry and [5]Argonne-Northwestern Solar Energy Research (ANSER) Center, Northwestern University, 2145 Sheridan Road, Evanston, IL 60208, USA

[2]Department of Chemical Sciences, University of Padova, Via Marzolo 1, Padova 35131, Italy

[3]Institute of Natural Sciences, Westlake Institute for Advanced Study, Westlake University, 18 Shilongshan Road, Hangzhou 310024, China

[4]Materials and Process Simulation Center, California Institute of Technology, Pasadena, CA 91125, USA

Supporting Information Placeholder

ABSTRACT: Herein, we report an unprecedented mixed-valence crystal superstructure which consists of a 2:1 host-guest complex $[MV\subset(CBPQT)_2]^{2/3+}$ [MV ≡ methyl viologen, CBPQT ≡ cyclobis(paraquat-*p*-phenylene)]. One electron is distributed statistically between three $[MV\subset(CBPQT)_2]^{\bullet+}$ comprised of a total of 15 viologen units. The mixed-valence state is validated by single-crystal X-ray crystallography which supports an empirical formula of $[MV\subset(CBPQT)_2]_3\bullet(PF_6)_2$ for the body-centered cubic superstructure. Electron paramagnetic resonance provides further evidence of electron delocalization. Quantum chemistry calculations confirm the mixed-valence state in the crystal superstructure. Our findings demonstrate that precise tuning of the redox states in host-guest systems can lead to a promising supramolecular strategy for achieving long-range electron delocalization in solid-state devices.

Long-range electron delocalization[1] involving noncovalently bonded assemblies plays a pivotal role in biological processes such as light-harvesting antenna complexes[2]. A steadily improving understanding of electron delocalization at the molecular level has been assisted by the investigation of artificial model systems—involving donor–acceptor assemblies[3-5] and mixed-valence complexes[6-8]—which have instigated the creation of optoelectronic devices. Indeed, tremendous advances have been made[7,9] towards developing artificial systems composed of molecular frameworks and supramolecular architectures. The development of host-guest chemistry has opened[10-11] the door to synthetic hosts being ideal systems for studying electron delocalization through noncovalent-bonding interactions. Since the late 1980s, we have investigated[12] cyclobis(paraquat-*p*-phenylene) ($CBPQT^{4+}$, Figure 1a)—composed of two 1,1′-dialkyl-4,4′-bipyridinium ($BIPY^{2+}$, Figure 1a) dicationic units—which is capable of forming inclusion complexes with neutral π-electron-rich guests through π–π and charge-transfer interactions. Recently, we discovered[13] the ability of $CBPQT^{4+}$, when reduced to $CBPQT^{2(\bullet+)}$, to form a stable 1:1 inclusion complex $BIPY^{\bullet+}\subset CBPQT^{2(\bullet+)}$ with appropriate guests containing $BIPY^{\bullet+}$ because of favorable radical–radical interactions[14-16]. By employing this 1:1 complex as a template, many high-energy mechanically interlocked molecules[17-18](MIMs)—which would otherwise be difficult to synthesize—have been prepared. These MIMs exhibit intramolecular electron delocalization in their mixed-valence states thanks to the protection of the mechanical bond.

Herein, we demonstrate an unprecedented example of mixed-valence states in a crystal superstructure assembled from a unique 2:1 host-guest complex $MV\subset(CBPQT)_2$ (MV ≡ methyl viologen)—namely, one MV entity encircled by two CBPQT rings—which bears evenly 2/3+ charge. In other words, two positive charges are distributed statistically among total 15 BIPY units assembled into two $MV^{\bullet+}\subset(CBPQT^0)_2$ and one neutral $MV^0\subset(CBPQT^0)_2$. The formation of this mixed-valence complex as well as its unusual ratio of BIPY/charge have been confirmed by single-crystal X-ray diffraction (XRD), which affords an empirical formula of $[MV\subset(CBPQT)_2]_3\bullet(PF_6)_2$ for the body-centered cubic superstructure, while the existence of free radicals in the bulk sample has been proved by electron paramagnetic resonance (EPR) spectroscopy. Quantum chemistry calculations support the existence of mixed-valence state.

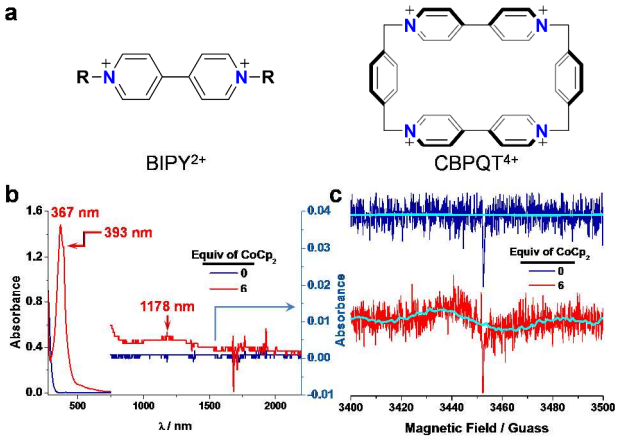

Figure 1. (a) Structural formulas of $BIPY^{2+}$ and $CBPQT^{4+}$. (b) UV-Vis-NIR Absorption and (c) EPR spectra of an equimolar mixture (deep blue) of $CBPQT\bullet4PF_6$ and $MV\bullet2PF_6$ and its reduced product (red) upon addition of 6 equiv of $CoCp_2$.

To understand the binding properties[19] of CBPQT^0 towards neutral MV^0, we investigated the reduction of an equimolar mixture of CBPQT•4PF$_6$ and MV•2PF$_6$ using cobaltocene ($CoCp_2$). The UV-Vis-NIR spectrum (Figure 1b) of this mixture before reduction exhibits no Vis-NIR absorption bands and no EPR signals are observed (Figure 1c). Upon reducing this mixture with 6 equiv of $CoCp_2$, a new band appears at 367 nm with a shoulder at 392 nm, observations which are in line with the spectra reported[19-20] for neutral CBPQT^0 and MV^0, indicating the generation of both these neutral forms. We observed, however, a very weak broad NIR absorption band at ~1178 nm, which is not really noticeable until it is magnified 20-fold. This characteristic NIR band, which de-rives from charge-resonance transitions, can be ascribed to the formation of complexes between BIPY^0 and trace of the incompletely reduced BIPY$^{•+}$ radical cations. Consistent with the appearance of the NIR band, a non-negligible weak EPR signal is also evident for the reduced solution sample, confirming the presence of radical species. The existence of both weak NIR band and EPR signal indicates that, although most of this mixture is reduced to CBPQT^0 and MV^0, trace amounts of BIPY in CBPQT or MV still remain as radical cationic BIPY$^{•+}$ which associates with its neutral counterpart BIPY^0. Thus, certain mixed-valence complexes are formed.

This observation encouraged us to assess the formation of complexes in the extreme case of a mixed-valence system. Despite the rapid disproportionation of BIPY$^{•+}$ radical cations, we were able to obtain black single crystals suitable for XRD from an equimolar mixture of CBPQT•4PF$_6$ and MV•2PF$_6$ reduced with 6 equiv of $CoCp_2$. The resulting black crystals are strikingly different from the red crystals of CBPQT^0 and MV^0. Single-crystal XRD analysis (Figure 2) shows that the superstructure is composed of a unique 2:1 host-guest complex MV⊂(CBPQT)$_2$—namely, a MV entity embraced by two CBPQT rings with a C_2 axis passing perpendicularly (Figure 2c) through the center of the MV plane. Two isostructural CBPQT rings—adopting a slightly conical shape with two angles between the ring plane and two *p*-xylene planes of 100 and 104°—are held (Figure 2b) together head–to–head by six [H···H] contacts of 2.33–2.39 Å. The "corner" angles of CBPQT are 112°, a value which is comparable with the 113° found in CBPQT^0. The mean distance between two BIPY planes of CBPQT is 6.83 Å, similar to the value reported[19] for CBPQT^0. The MV entity is encapsulated through π–π interactions of 3.31 Å between MV and two CBPQT as well as by four [C–H···π] interactions of 2.85–2.94 Å with a dihedral angle between MV and CBPQT of 70°. Somewhat unexpectedly, the positive charge carried by this complex is observed to be a non-integer less than one—namely, $[MV⊂(CBPQT)_2]^{2/3+}$—based on the average number of PF_6^- associated with each complex, indicating that statistically every two positive charges are distributed over three MV⊂(CBPQT)$_2$ complexes comprised of a total of 15 BIPY units. This $[MV⊂(CBPQT)_2]^{2/3+}$ complex is unprecedented on account of the fact that there are no examples of (i) one aromatic guest encircled by two CBPQT rings and (ii) a host-guest complex bearing charges more than zero but less than one.

Despite the fact that torsional angles associated with BIPY change upon guest complexation, the change in the bond lengths can be used to establish[19,21-22] the oxidation states of BIPY. To clarify the oxidation states of each BIPY of $[MV⊂(CBPQT)_2]^{2/3+}$, we compared the bond lengths of two classes of BIPY units in this complex with those for BIPY reportedly[19,23] present in CBPQT^{4+}, CBPQT$^{2(•+)}$, and CBPQT^0 as well as MV^{2+}, MV$^{•+}$, and MV^0. We were able to identify (Figure 3) a clear trend in the lengths of the bonds in BIPY at different redox states. In particular, the bond length for C4–C4′ undergoes a distinct change from ~1.49 Å (2+), to ~1.43 Å (•+), to ~1.37 Å (0), in line with the nature of bond C4–C4′ changing from a single bond, a radical-delocalized bond,

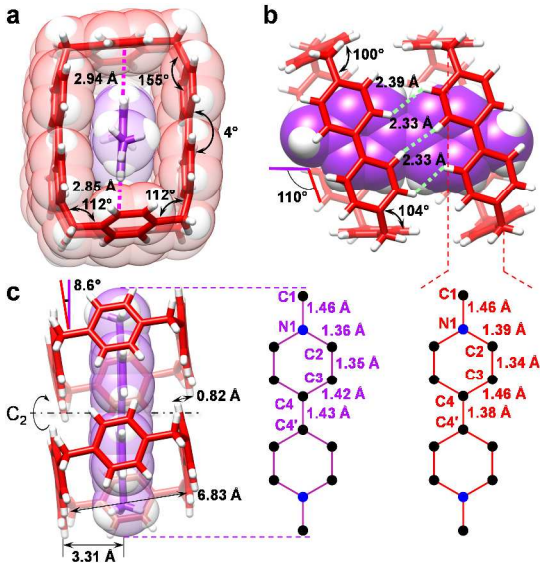

Figure 2. Crystal (super)structure of MV⊂(CBPQT)$_2$. (a) Front view showing the corner angles of CBPQT, torsional angle of BIPY in CBPQT, and [C–H···π] interactions (pink dash lines). (b) Side view exhibiting the angles between xylene planes and CBPQT, the dihedral angle between MV and CBPQT, and [H···H] interactions (blue dash lines) between two CBPQT. (c) Top view indicating the C_2 symmetrical axis and the width of CBPQT, and π–π interactions between MV and CBPQT. H, white; CBPQT, red; MV, purple. The bond lengths of BIPY in MV and CBPQT are portrayed in purple and red, respectively.

to a double bond. Based on this regularity, we found that the bond lengths of BIPY for CBPQT in MV⊂(CBPQT)$_2$ match well with those reported for BIPY of CBPQT^0 and MV^0, indicating that CBPQT in MV⊂(CBPQT)$_2$ is in its neutral CBPQT^0 state. On the other hand, the bond lengths for MV in MV⊂(CBPQT)$_2$ are comparable with those of BIPY$^{•+}$ in CBPQT$^{2(•+)}$ and MV$^{•+}$, suggesting the radical cationic MV$^{•+}$ state of MV. Bond-length analysis indicate that most of MV⊂(CBPQT)$_2$ are likely in their mixed-valence state MV$^{•+}$⊂(CBPQT^0)$_2$ on account of the formula of $[MV⊂(CBPQT)_2]^{2/3+}$ of the complex.

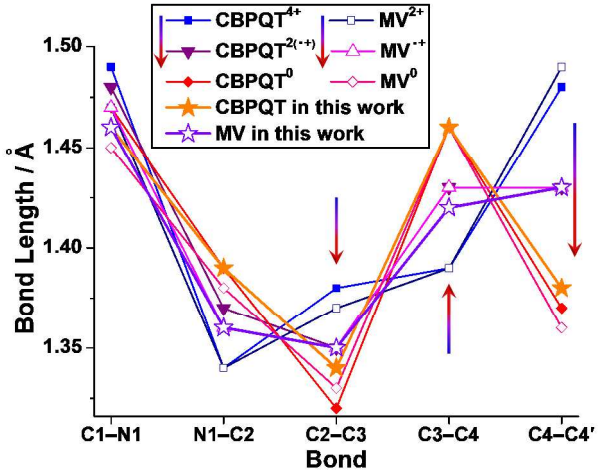

Figure 3. Comparison of bond lengths of BIPY in MV and CBPQT for MV⊂(CBPQT)$_2$ with BIPY in CBPQT^{4+}, CBPQT$^{2(•+)}$, CBPQT^0, MV^{2+}, MV$^{•+}$, and MV^0. Arrows indicate the changes in bond lengths of BIPY.

The existence of the unpaired electrons in the mixed-valence crystals was also confirmed by EPR spectroscopy. An EPR signal inhomogeneously broadened by many hyperfine splittings was

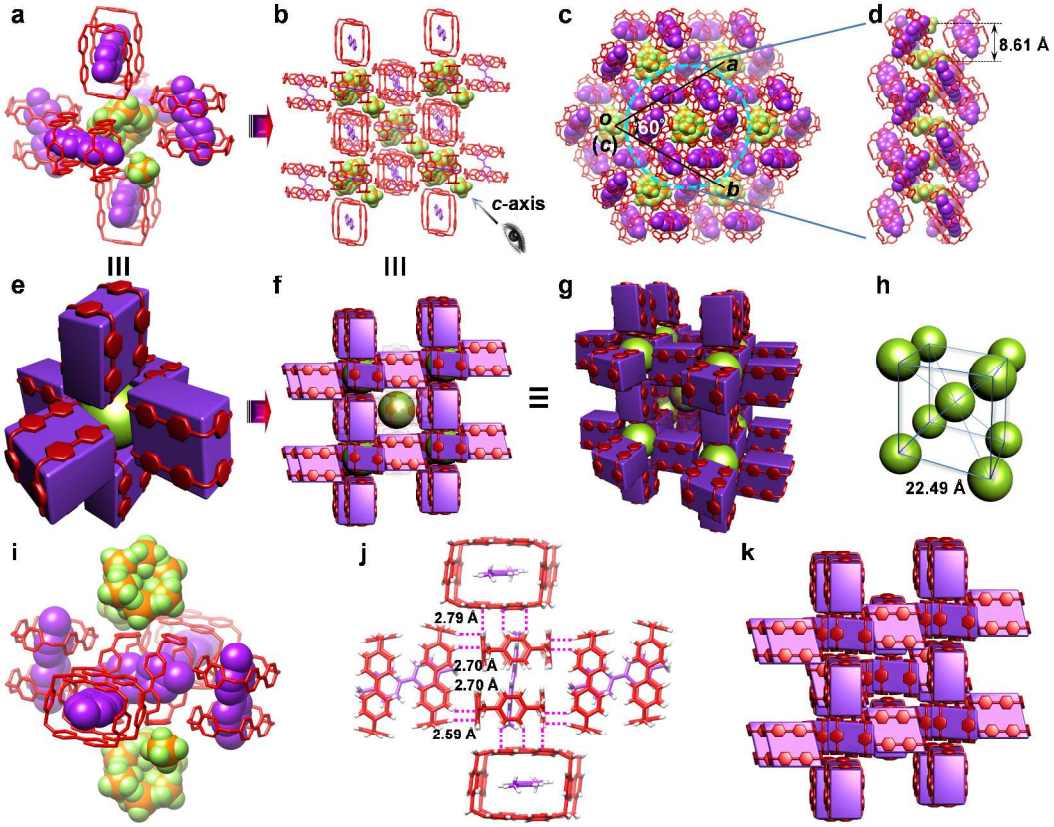

Figure 5. Crystal superstructure of $[MV\subset(CBPQT)_2]_3\bullet(PF_6)_2$. (a) Octahedron assembled from six $MV\subset(CBPQT)_2$ surrounding two PF_6^- and (e) its schematic representation. (b) Body-centered cubic superstructure assembled by adjacent octahedrons sharing $MV\subset(CBPQT)_2$ as linkers and (f and g) its schematic representations. (d) Hexagonal channels packing into (c) hexagonal arrangement as viewing along *c*-axis (the diagonal of the cube in b). (h) Schematic representation of body-centered cubic superstructure after removing all $MV\subset(CBPQT)_2$. Green balls represent PF_6^- pairs in e-h. (i) A representation showing that every $MV\subset(CBPQT)_2$ is encircled by four $MV\subset(CBPQT)_2$ and two pairs of PF_6^-. (j) 20 Complementary [C–H···π] interactions (Figure S2) of 2.59–2.79 Å between BIPY planes and H atoms on CBPQT of adjacent $MV\subset(CBPQT)_2$. (k) Schematic representation of an extended body-centered cubic framework wherein PF_6^- pairs are omitted. CBPQT, red; MV, purple; F, green; P, yellow. H atoms in a-d and i and solvents are omitted.

obtained (Figure 4) on a crystalline sample, and had *g*-factor similar to those reported[19] for mixed-valence $BIPY^{\bullet+}$-containing solid-state samples, indicating the presence of free radicals in the solid-state superstructure. Since no single $MV\subset(CBPQT)_2$ bears statistically one full positive charge based on the empirical formula of $[MV\subset(CBPQT)_2]_3\bullet(PF_6)_2$, we believe that the unpaired electron is delocalized inside $[MV\subset(CBPQT)_2]^{\bullet+}$.

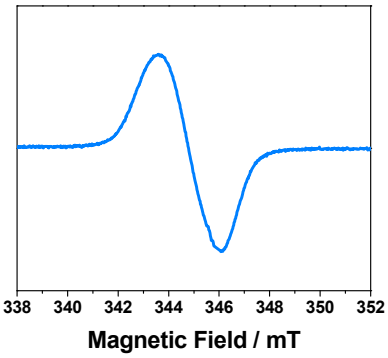

Figure 4. Solid-state continuous-wave EPR spectrum of crystals of $[MV\subset(CBPQT)_2]_3\bullet(PF_6)_2$.

The X-ray crystal superstructure reveals that every two PF_6^- anions—one of them disordered (Figure S1) about a six-fold *c*-axis—are surrounded by the *para*-xylylene planes of six $MV\subset(CBPQT)_2$ to form (Figure 5a and e) an octahedron wherein six $MV\subset(CBPQT)_2$ occupy the vertices, but they also serve as shared linkers in connecting these octahedrons together in a three-dimensional array which extends throughout the whole crystal. Thus, every octahedron has the empirical formula of $[MV\subset(CBPQT)_2]_3\bullet(PF_6)_2$. The $[MV\subset(CBPQT)_2]_3\bullet(PF_6)_2$ repeating motifs adopt (Figure 5b, f-g) an approximately body-centered cubic packing arrangement, wherein (i) PF_6^- anion pairs represent (Figure 5h) the vertices and the center of the cube and (ii) each $MV\subset(CBPQT)_2$ is linked with two pairs of PF_6^- through its two outward-pointing *para*-xylylene faces. As viewed along the *c*-axis (Figure 5b), hexagonal channels—which are filled (Figure 5d) up with PF_6^- anions at 8.61 Å apart from each other and penetrate through every octahedron—can be observed to pack (Figures 4c and S1) into a hexagonal arrangement. In the superstructure every $MV\subset(CBPQT)_2$ is encircled (Figure 5i) by four adjacent $MV\subset(CBPQT)_2$ and two pairs of PF_6^- generating an octahedron. Since every complex has three types of facets—namely, *para*-xylylene planes, BIPY planes, and CBPQT ring planes—in which the *para*-xylylene planes interact with PF_6^- anions, every $MV\subset(CBPQT)_2$ links (Figures 5j and S2) with four adjacent but orthogonally oriented $MV\subset(CBPQT)_2$ by means of 20 complementary [C–H···π] interactions ranging from 2.59 to 2.79 Å between the BIPY planes and H atoms on the CBPQT rings, assembling (Figure 5k) into an extended body-centered cubic framework with PF_6^- pairs as vertices and center of each cube. Hirshfeld surface analysis confirms[24] (Figure S2b) that the reciprocal [C–H···π]/[π···H–C] interactions, which contribute 79.8%, are the most significant interactions between $MV\subset(CBPQT)_2$

units. This extended superstructure can be a result of the even distribution of the positive charges throughout the whole crystal.

Quantum chemistry calculations were carried out to analyze the charge distribution within and beyond MV⊂(CBPQT)$_2$ in the solid state. The optimized unit cell contains (Figure S3) three MV⊂(CBPQT)$_2$ (**a**, **b** and **c**) and two PF_6^-. Mulliken-charge and spin-population analyses of both MV⊂(CBPQT)$_2$ and MV show (Table S2) that the two positive charges are not evenly distributed in the three MV⊂(CBPQT)$_2$ but are localized on two $MV^{\bullet+}$⊂(CBPQT^0)$_2$ with one neutral MV^0⊂(CBPQT^0)$_2$. The calculated bond lengths (Table S2) for C4–C4′ in MV^0 (1.36 Å) and $MV^{\bullet+}$ (1.42 Å) agree well with the trend in Figure 3. The uneven distribution of positive charge attracts PF_6^- anions, encouraging one of them to drift from the 3-fold axis to a position that is closer to the two $MV^{\bullet+}$⊂(CBPQT^0)$_2$. Such an outcome is in agreement with observations (from XRD) which show that one of the two PF_6^- anions does not occupy one single position with equal distances between six MV⊂(CBPQT)$_2$, but is disordered over six symmetry-related positions with one-sixth occupancy.

We have demonstrated that two CBPQT rings are able to encapsulate cooperatively one MV entity to form a mixed-valence 2:1 host-guest complex MV⊂(CBPQT)$_2$. XRD analysis indicates that every three MV⊂(CBPQT)$_2$ share statistically two positive charges to give a body-centered cubic superstructure with the empirical formula of [MV⊂(CBPQT)$_2$]$_3$•(PF$_6$)$_2$. The fact that every MV⊂(CBPQT)$_2$ bears only a mean charge of 2/3+ suggests the distribution of every two positive charges over two $MV^{\bullet+}$⊂(CBPQT^0)$_2$ with one neutral MV^0⊂(CBPQT^0)$_2$. Quantum chemistry calculations confirm the mixed-valence state of the solid-state superstructure. This research highlights the potential of host-guest strategies for achieving long-range charge delocalization in solid-state devices by constructing host-guest complexes with precisely adjustable redox states.

ASSOCIATED CONTENT

Supporting Information

Detailed information regarding the experimental methods and procedures, X-ray crystallographic data, and supportive figures and tables. This material is available free of charge via the Internet at http://pubs.acs.org. CIF file for [MV⊂(CBPQT)$_2$]$_3$•(PF$_6$)$_2$ (CCDC 985866).

AUTHOR INFORMATION

Corresponding Authors

zhichang-liu@northwestern.edu
stoddart@northwestern.edu

Notes

The authors declare no competing financial interests.

ACKNOWLEDGMENT

This research is part of the Joint Center of Excellence in Integrated Nano-Systems (JCIN) at the King Abdulaziz City for Science and Technology (KACST) and Northwestern University (NU). The authors thank both KACST and NU for their continued support of this research. This research was also supported by the National Science Foundation under grant no. DMR-1710104 (M.R.W.).

REFERENCES

(1) Winkler, J. R.; Gray, H. B. *J. Am. Chem. Soc.* **2014**, *136*, 2930.
(2) McDermott, G.; Prince, S. M.; Freer, A. A.; Hawthornthwaite-Lawless, A. M.; Papiz, M. Z.; Cogdell, R. J.; Isaacs, N. W. *Nature* **1995**, *374*, 517.
(3) Zhu, W.; Zheng, R.; Fu, X.; Fu, H.; Shi, Q.; Zhen, Y.; Dong, H.; Hu, W. *Angew. Chem. Int. Ed.* **2015**, *54*, 6785.
(4) Murase, T.; Otsuka, K.; Fujita, M. *J. Am. Chem. Soc.* **2010**, *132*, 7864.
(5) Park, J. S.; Karnas, E.; Ohkubo, K.; Chen, P.; Kadish, K. M.; Fukuzumi, S.; Bielawski, C. W.; Hudnall, T. W.; Lynch, V. M.; Sessler, J. L. *Science* **2010**, *329*, 1324.
(6) Leblanc, N.; Mercier, N.; Toma, O.; Kassiba, A. H.; Zorina, L.; Auban-Senzier, P.; Pasquier, C. *Chem. Commun.* **2013**, *49*, 10272.
(7) Hankache, J.; Wenger, O. S. *Chem. Rev.* **2011**, *111*, 5138.
(8) Yoshizawa, M.; Kumazawa, K.; Fujita, M. *J. Am. Chem. Soc.* **2005**, *127*, 13456.
(9) Lindeman, S. V.; Rosokha, S. V.; Sun, D.; Kochi, J. K. *J. Am. Chem. Soc.* **2002**, *124*, 843.
(10) Berville, M.; Karmazin, L.; Wytko, J. A.; Weiss, J. *Chem. Commun.* **2015**, *51*, 15772.
(11) Ko, Y. H.; Kim, E.; Hwang, I.; Kim, K. *Chem. Commun.* **2007**, 1305.
(12) Odell, B.; Reddington, M. V.; Slawin, A. M. Z.; Spencer, N.; Stoddart, J. F.; Williams, D. J. *Angew. Chem. Int. Ed.* **1988**, *27*, 1547.
(13) Trabolsi, A.; Khashab, N.; Fahrenbach, A. C.; Friedman, D. C.; Colvin, M. T.; Cotí, K. K.; Benítez, D.; Tkatchouk, E.; Olsen, J.-C.; Belowich, M. E.; Carmielli, R.; Khatib, H. A.; Goddard, W. A., III; Wasielewski, M. R.; Stoddart, J. F. *Nat. Chem.* **2010**, *2*, 42.
(14) Geraskina, M. R.; Dutton, A. S.; Juetten, M. J.; Wood, S. A.; Winter, A. H. *Angew. Chem. Int. Ed.* **2017**, *56*, 9435.
(15) Sakai, F.; Ji, Z.-W.; Liu, J.-H.; Chen, G.-S.; Jiang, M. *Chin. Chem. Lett.* **2013**, *24*, 568.
(16) Chen, L.; Zhang, Y.-C.; Wang, W.-K.; Tian, J.; Zhang, L.; Wang, H.; Zhang, D.-W.; Li, Z.-T. *Chin. Chem. Lett.* **2015**, *26*, 811.
(17) Li, H.; Zhu, Z.; Fahrenbach, A. C.; Savoie, B. M.; Ke, C.; Barnes, J. C.; Lei, J.; Zhao, Y.-L.; Lilley, L. M.; Marks, T. J.; Ratner, M. A.; Stoddart, J. F. *J. Am. Chem. Soc.* **2013**, *135*, 456.
(18) Sun, J.; Liu, Z.; Liu, W.-G.; Wu, Y.; Wang, Y.; Barnes, J. C.; Hermann, K. R.; Goddard, W. A., III; Wasielewski, M. R.; Stoddart, J. F. *J. Am. Chem. Soc.* **2017**, *139*, 12704.
(19) Frasconi, M.; Fernando, I. R.; Wu, Y.; Liu, Z.; Liu, W.-G.; Dyar, S. M.; Barin, G.; Wasielewski, M. R.; Goddard, W. A., III; Stoddart, J. F. *J. Am. Chem. Soc.* **2015**, *137*, 11057.
(20) Bockman, T. M.; Kochi, J. K. *J. Org. Chem.* **1990**, *55*, 4127.
(21) Porter, W. W.; Vaid, T. P.; Rheingold, A. L. *J. Am. Chem. Soc.* **2005**, *127*, 16559.
(22) Ivanov, M. V.; Wang, D.; Navale, T. S.; Lindeman, S. V.; Rathore, R. *Angew. Chem. Int. Ed.* **2018**, *57*, 2144.
(23) Fahrenbach, A. C.; Barnes, J. C.; Lanfranchi, D. A.; Li, H.; Coskun, A.; Gassensmith, J. J.; Liu, Z.; Benítez, D.; Trabolsi, A.; Goddard, W. A., III; Elhabiri, M.; Stoddart, J. F. *J. Am. Chem. Soc.* **2012**, *134*, 3061.
(24) Turner, M. J.; McKinnon, J. J.; Wolff, S. K.; Grimwood, D. J.; Spackman, P. R.; Jayatilaka, D.; Spackman, M. A. *CrystalExplorer17*; University of Western Australia, 2017.

Insert Table of Contents artwork here